Biomimetic Nerve Scaffolds with Aligned Intraluminal Microchannels: A "Sweet" Approach to Tissue Engineering

Jianming Li,[†] Todd A. Rickett,[†,§] and Riyi Shi*[,†,‡]

Weldon School of Biomedical Engineering, Purdue University, West Lafayette, Indiana 47907, Department of Basic Medical Sciences, Purdue University, West Lafayette, Indiana 47907, and Indiana University School of Medicine, Indianapolis, Indiana 46202

Received October 22, 2008. Revised Manuscript Received November 28, 2008

In this paper, we outline a method for the fabrication of biomimetic hollow fiber and hollow fiber bundles with high aspect ratios. The manufacturing process utilizes a melt spinning technique with caramelized sucrose as a core template. Encapsulation of the sucrose with a thin layer of degradable polymer and selective dissolution of the sucrose core produced tubes and tube aggregates with geometries similar to biologic analogs. The manufacturing process requires no specialized equipment and minimal quantities of organic solvent/polymer. These scaffolds were shown to induce nerve and glial cell alignment *in vitro* and may be further customized to integrate with other tissue or cell culture systems.

Introduction

Nature represents a plentiful source of unique and elegant structures. One ubiquitous form is the thin walled tubule. Tubule architectures are recurring thematic elements as mechanisms of transport as well as hierarchal ensheathment structures. For instance, animal capillaries and vascular tissue in plants resemble single or aggregate tubules, while skeletal muscle, ligaments and peripheral nerve are organized into repeating units enclosed in sheath layers. From a bioengineering perspective, these bundled tubule geometries have spawned significant interest, especially in regenerative medicine. However, due to the exceedingly high aspect ratios and thin walled characteristics, manufacture has been a challenge.[1−3] Previous techniques such as thermally induced phase separation, mandrel coating, excimer laser, CAD/CAM based molding have been used to generate tube-like formations.[3−7] Most of these procedures represent a "brute force" solution and in many cases do not yield adequate void space for tissue infiltration. In other techniques such as thermal phase separation, the tubules are only continuous through a narrow length scale. The invested time and equipment is also of concern. The alternative method commonly used to obtain endogenous tissue architecture is acellularization of allografts or xenografts.[8,9] However, acellularized constructs have limited customization potential, possible antigenicity, or may be the source of human/zoonotic disease.

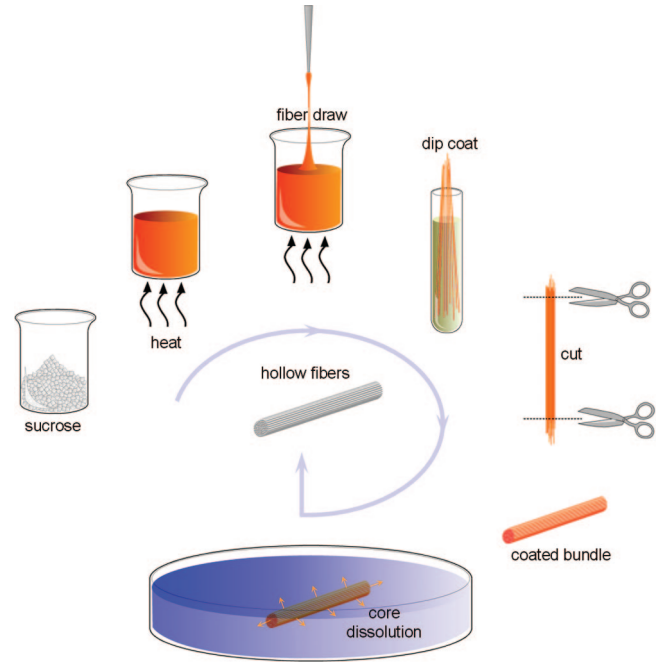

Figure 1. Fabrication of hollow fiber and hollow fiber bundles via melt spinning and selective dissolution. Granulated sucrose was initially heated to carmelization temperature and then cooled to a viscous state (125 °C). A dipping micropipette was then placed into the melt and drawn at a rate of ∼1 m/s. Fibers were subsequently air cooled, cut and sorted by length. Individual or multiple fibers were momentarily placed in a 2% w/v PLLA/chloroform solution and withdrawn. Coated fibers were then placed in an oven (37 °C) to remove residual solvent and trimmed to size. Sucrose core dissolution was accomplished via immersion of the coated fibers in distilled water.

Here we present a minimalist approach for the manufacture of customizable single and arrayed tubular scaffolds comparable to structures found *in vivo*. The proposed method consumes minimal resources and reduces preparation to a time scale of minutes. The fabrication process can be condensed into three primary stages: (i) creation of fiber core (template) and (ii) polymeric coating and (iii) selective dissolution of the core (Figure 1). The novelty of the technique comes from the utilization of caramelized table sugar (sucrose) as the template base. While

* Corresponding author. E-mail: riyi@purdue.edu.
[†] Weldon School of Biomedical Engineering, Purdue University.
[§] Indiana University School of Medicine.
[‡] Department of Basic Medical Sciences, Purdue University.

(1) Bender, M. D.; Bennett, J. M.; Waddell, R. L.; Doctor, J. S.; Marra, K. G. *Biomaterials* **2004**, *25*(7−8), 1269–1278.
(2) Fields, R. D.; Le Beau, J. M.; Longo, F. M.; Ellisman, M. H. *Prog. Neurobiol.* **1989**, *33*(2), 87–134.
(3) Ma, P. X.; Zhang, R. *J. Biomed. Mater. Res.* **2001**, *56*(4), 469–477.
(4) Brayfield, C. A.; Marra, K. G.; Leonard, J. P.; Tracy Cui, X.; Gerlach, J. C. *Acta Biomater.* **2008**, *4*(2), 244–255.
(5) Sundback, C.; Hadlock, T.; Cheney, M.; Vacanti, J. *Biomaterials* **2003**, *24*(5), 819–830.
(6) Widmer, M. S.; Gupta, P. K.; Lu, L.; Meszlenyi, R. K.; Evans, G. R.; Brandt, K.; Savel, T.; Gurlek, A.; Patrick, C. W., Jr.; Mikos, A. G. *Biomaterials* **1998**, *19*(21), 1945–1955.
(7) Stokols, S.; Tuszynski, M. H. *Biomaterials* **2006**, *27*(3), 443–451.
(8) Udina, E.; Voda, J.; Gold, B. G.; Navarro, X. *J. Peripher. Nerv. Syst.* **2003**, *8*(3), 145–154.
(9) Keilhoff, G.; Pratsch, F.; Wolf, G.; Fansa, H. *Tissue Eng.* **2005**, *11*(7−8), 1004–1014.

10.1021/la803522f CCC: $40.75
Published on Web 12/24/2008

particulate sucrose is a commonly used porogen, tubules originating from sucrose cores have not been studied at the microscale. Therefore, this research provides proof of concept for using shaped sucrose as templates for more organized structures. We believe this strategy could be invaluable to scaffold engineering by facilitating the development of complex, ordered constructs capable of supporting cell growth.

The initial step in the manufacturing process begins by obtaining desired microfibers as a template source. Microfibers were created by first heating granulated sucrose to caramelization temperatures (>200 °C). This process induces a browning reaction and creates a byproduct suitable for manipulation (note that the melt consists of higher molecular weight sugars, ketones, carmelins and other compounds, but for simplicity, this cocktail of organics will we termed "sucrose fiber" henceforth).[10] Next, a glass micropipette was placed into the sucrose melt and withdrawn at rates of 0.3−1.0 m/s. With this spinning method, fibers on the range of 8−100 μm in diameter and lengths in the tens of centimeters (l/d aspect ratios up to 10^4) were realized. The thinnest fibers were obtained by using a small spinneret (tip radius 200 μm), faster draw rates and reduced melt viscosity (more thorough mathematical descriptions of this spinning process can be obtained in Middleman).[11] The formed fibers possessed unique physical properties that make them well suited for manipulation. While glassy sucrose has a high modulus, low fiber stiffness was achieved due to thin fibril diameters. Fiber templating also offers other advantages since fiber properties such as diameter, wall thickness, surface roughness, porosity can be controlled individually during spinning.

Following the spinning process, sucrose fibers were encapsulated by brief exposure (dipping) into a 2% poly l-lactic acid (PLLA)/chloroform solution. Coated fibers were then air-dried to remove residual solvent. Currently, we used PLLA and chloroform as the working system. Chloroform is a good solvent of PLLA but a poor solvent of polar sucrose. This disparity in solubility permits the use of liquid based coatings without affecting the underlying sucrose structure. Finally, the sucrose core was removed by immersion in distilled water (Figure 2b). Core dissolution of a typical tubule was captured with time-lapse cinematography (Supporting Information video). Exposure of the PLLA coated sucrose fibers to distilled water resulted in rapid solute outflow. The majority of the sugar core diffused across the wall within 30 s and in certain locations along the tubule axis, small particulates were observed migrating across the wall boundary. Scanning electron micrographs of the tubules depict smooth surfaces punctuated by random pores (Figure 2c−e). This topography was confirmed with contact mode atomic force microscopy (AFM), as the smooth wall regions resulted in a surface roughness (R_a) of less than 2 nm (Figure 2f). Analysis of pore size distribution revealed a tendency toward submicrometer diameters, with a mean pore diameter of 297.3 ± 132.4 nm (n = 137, Figure 2f). The area pore density was found to be 9400 ± 15000/mm^2. The pore data lends insight into the screening selectivity of the tubules. Smaller submicrometer particles can readily diffuse across the boundaries while transmembrane transport of larger objects is inhibited. This is a notable modification since bulk PLLA has a low gas permeability, resembling polyethylene terephthalate (PET) and polystyrene (PS).[12] This increased permeability is especially desirable in biologic applications where nutrient and waste exchange are paramount.

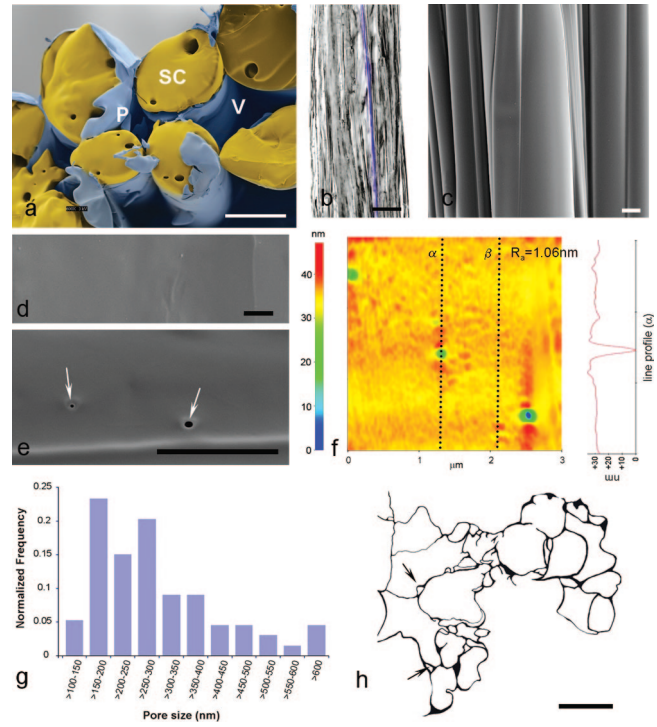

Figure 2. (a) Enlarged SEM micrograph of undissolved PLLA tubule cross sections obtained via freeze-fracture. The image shows the sucrose core (denoted SC and pseudocolored yellow) as well as the PLLA sheath (denoted P and pseudocolored blue). The multiple tubules form an aggregate bundle with individually distinct members. Smaller channels (denoted V) formed by nonintersecting walls are also shown. (b) phase contrast image of the PLLA constructs in PBS. The pseudoblue tinting delineates a single tubule. (c) An SEM profile view of tubular constructs. Photomicrographs of the tubule lumen (d) and exterior (e) depict flat regions populated with rounded pores. (f) AFM measurements of the PLLA surfaces confirm the SEM data, demonstrating flat zones (surface roughness, R_a < 2 nm, along β line trace) punctuated with spatially random pores. Right: Corresponding line profile along a line trace. (g) Pore size distribution data show a mean pore diameter of 297.3 ± 132.4 nm and a pore range of 138 − 570 nm (n = 137). (h) Cross sectional tracings obtained from phase contrast microscopy are shown. The cropped image confers a significant degree of interconnectedness between tubules. Wall thickness was as small as 1 μm. Black arrows highlight channels formed by voids between tubules (denoted V in part a). The irregular shapes represent an instantaneous capture of the tubules and do not necessarily reflect the permanent architecture since the tubules are highly flexible. Scale: (a) 40 μm, (b) 500 μm, (c−e) 10 μm, and (h) 50 μm.

Additional cross sectional scans of PLLA tubules analyzed with SEM and optical microscopy revealed individual tubes with external diameters on the order of 8−100 μm. Tube wall were generally between 0.75−3 μm thick in single tube entities, but this property is tunable by varying the PLLA concentration. Bundles were assembled by stacking fibers prior to core dissolution. Aggregating individually coated fibers yielded fully closed channels, with small voids between adjacent tubules (Figure 2a,h). The cross-sectional transparency was also high, with the bulk polymer occupying less than 13% of the total enclosed area (Figure 2h). Note that dissolution of the solid core resulted in an irregular but compliant PLLA matrix. We also attempted dip coating groups (~100−200 fibers) of sucrose fibers simultaneously into the polymer solution, but this technique created a mixture of open and closed channel architectures. Assembled bundles generally had walls approximately 1−2 μm in thickness. In nodal regions, where walls intersect, thicknesses

(10) Kitts, D. D.; Wu, C. H.; Kopec, A.; Nagasawa, T. *Mol. Nutr. Food Res.* **2006**, *50*(12), 1180–1190.
(11) Middleman, S., Chapter 9: Fiber Spinning. In *Fundamentals of Polymer Processing*, 1st ed.; McGraw-Hill: New York, 1977.
(12) Auras, R. A.; Harte, B.; Selke, S.; Hernandez, R. J. *J. Plastic Film Sheeting* **2003**, *19*(2), 123.

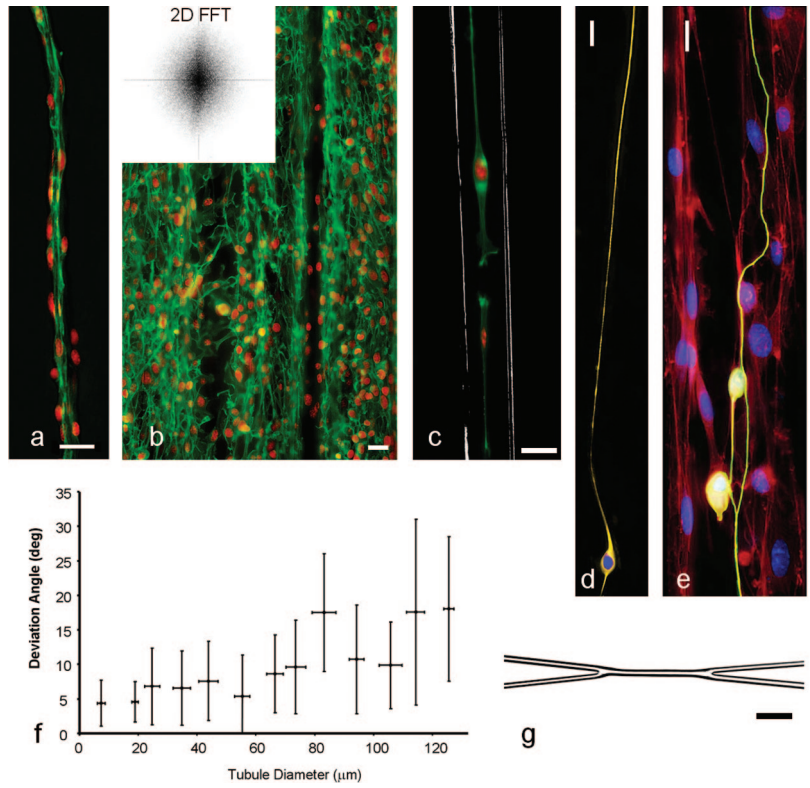

Figure 3. (a) Immunostained image of rat Schwann cells cultured onto a single 8 μm diameter PLLA tubule. At this size scale, the cells were observed to attach and align only along the exterior surface. The Actin cytoskeleton (green) was stained with phalloidin-AlexaFluor 488 and nuclei (red) were labeled with propidium iodide (with RNase A digestion). (b) Schwann cells cultured onto larger diameter tubule bundles depict aligned morphologies. Inset: A 2-D FFT (rotated 90 °CW) plot of (b) shows spatial features coincident with the long axis of the tubules. High frequency components as well as lower frequency elements were observed to have directional preferences. (c) Growth of cells strictly within tubules was characterized with a specialized cell culture system. Merged phase contrast and fluorescent images depict oriented Schwann cell alignment within a 25 μm diameter PLLA tubule. (d) Neurofilaments (yellow) of dissociated chick DRG cells regenerated (after 48 h) parallel to the tubule lumen. The nucleus was visualized with propidium iodide (blue). (e) A 24 h coculture of chick DRG and Schwann cells further validate controlled cell patterning with PLLA tubules. Neuronal processes were observed to follow the underlying Schwann cell topography. (f) Angular deviation of Schwann cell alignment as a function of tubule diameter (measured with respect to long axis). The data shows a correlation between deviation angle and tubule diameter ($R = 0.18$, $n = 245$). (g) Heat fused sucrose fibers demonstrate ease of manipulation and potential for various customized shapes. Scale: (a)-(e) 25 μm, (g) 25 μm.

were higher, generally approaching 5 μm. Thus, for maximum control of desired properties, tubules should be fabricated individually (or in parallel) and assembled.

The proposed polymer scaffolds have diverse tissue engineering and cell culture applications, but the primary focus was use in peripheral nerve regeneration. To demonstrate biological relevance, hollow fiber and fiber bundles were sterilized in ethanol and incubated with laminin. Schwann cells obtained from a Schwannoma cell line (ATCC) were subsequently seeded onto the scaffolds at a density of 1.0×10^4 cells/cm^2 (see Experimental Methods). Cells followed typical growth curve characteristics and during the proliferation phase, daughter cells readily adhered and migrated along the tubule surfaces. After 3−4 days in culture, the Schwann cells reached confluence and were stained with DNA (propidium iodide, red, Figure 3a) and Actin markers (AlexaFluor conjugated-phalloidin, green, Figure 3a). Growth was visualized on both the exterior and interior (lumenal) surfaces of the tubules (Figure 3a,b). Adherent Schwann cells possessed an elongated morphology with processes extending parallel to the fiber direction. The degree of alignment was characterized with 2-D fast Fourier transform (FFT). In the FFT data, Actin (higher frequency components) and cell nuclei (lower frequency) elements contributed to an elliptical distribution plot, with the major axis corresponding with the tubule direction[13] (Figure 3b). Thus, a preferred orientation was evident at the whole cell and at the subcellular level. Moreover, direct measurement of the cell morphology was conducted by tracing individual cells. These cell orientation plots confer a positive correlation ($p < 0.001$, $r = 0.18$) between cell alignment and tubule diameter (Figure 3f). The decreased variability in cell orientation angles at smaller tubule diameters provides insight in designing scaffolds with optimal contact guidance properties. Indeed, measured cell angles show less than 10° average deviation in tubule widths of 50 μm or less.

In addition, primary neurons harvested from chick dorsal root ganglia (DRG) extended neurites along the tubule direction (Figure 3d). The DRGs exhibited relatively straight growth trajectories. To simulate *in vivo* conditions, cocultures of DRGs overlaid on Schwann cell monolayers were also evaluated. Both cell types were found to be coincident with the tubule axis (Figure 3e). Neuronal processes navigated via a combination of guidance cues provided by the Schwann cell subculture as well as the tubule surface. This finding is comparable to neuron-glia cultures grown on micropatterned substrates[14] and suggests another method for dictating cell orientation. In specific neural applications

(13) Ayres, C. E.; Jha, B. S.; Meredith, H.; Bowman, J. R.; Bowlin, G. L.; Henderson, S. C.; Simpson, D. G. *J. Biomater. Sci. Polym. Ed.* **2008**, *19*(5), 603–621.

such as peripheral nerve regeneration, this ability to facilitate axon pathfinding is essential in minimizing aberrant regeneration.[15]

Finally, the unique physiochemical properties of sucrose hold promise for templating tissue scaffolds. The reported manufacturing process is robust and amenable to the inclusion of bioactive domains (cytokines, anti-inflammatory agents, etc.) within a polymer monolith. Additionally, individual fibers can also be fused/shaped by reheating to the glass transition temperature or by exposure to moisture (>50% relative humidity atmosphere, 25 °C, Figure 3g). The corresponding geometries can be applied to simple microfluidic or tissue culture platforms (such as paralleled channeled Campenot chambers[16]) without traditional microfabrication facilities. And by migrating fiber creation to a parallel process, a significant number of custom tailored units can also be realized. While we report templating sucrose with PLLA, other polymer systems such as tissue culture polystyrene/chloroform are also compatible. Spray coating may further be substituted for dip coating. Thus, the reported technique supplements current manufacturing schemes but with added simplicity, low-cost and reduction in environmentally harmful chemicals.

Experimental Methods

Tubule Formation. Granulated sucrose was heated (215 °C) in a stainless steel pan to initiate sucrose oxidation (caramelization). After several minutes of maintained heating, all sucrose particulates were caramelized, leaving a dark brown colored melt. The residual liquid was then cooled to the glass transition temperature (∼110 °C). Glass micropipettes (200 μm tip radius) were next placed into the viscous sugar and drawn at a rate of approximately 0.35 m/s. Pulled sucrose fibers (∼25−40 μm diameter) were air-cooled and cut. In single tubule formation, individual fibers were dipped into a solution of poly l-lactic acid (PLLA) and chloroform (2% w/v). For fiber bundle formation, multiple sugar fibers (∼100−200) arranged in a parallel array were simultaneously coated with PLLA solution. Through cohesive forces sucrose fibers self-organized into a tightly bound cable. Fibers were then placed in an oven (37 °C) overnight to remove residual solvent. The PLLA-sugar composites were then cut at the ends and placed in distilled water for core dissolution. Hollow fiber conduits were sterilized with 70% ethanol overnight.

Cell Culture and Immunocytochemistry. For cell culture, hollow fiber bundles were first immersed in a laminin (10 μg/mL in PBS) solution. In addition, the laminin liquid was circulated into the microtubules by repeated "pumping" with a pipet (pipet tip placed at the mouth of the constructs). The bundles were further incubated in the laminin solution overnight (37 °C). Rat Schwann cells derived from the RT4-D6P2T Schwannoma line (ATCC) were subsequently seeded onto the scaffolds at a density of 1.0×10^4 cells/cm^2. After 3−4 days of culture in DMEM, the Schwann cells reached confluence, whereby the cells were fixed with 4% paraformaldehyde (20 min.). Cells were then permeabilized with 0.1% Triton X-100 (5 min), rinsed three times with PBS and incubated with RNase A (100 μg/mL) for 20 min. DNA was labeled with propidium iodide (0.05 mg/mL, Sigma) exposure for 5 min. Actin microfilaments were marked with phalloidin conjugated AlexaFluor 488 (diluted 1:75, Invitrogen) incubated for 20 min. For primary cell culture, dorsal root ganglia were dissected from 7−8 day old chick embryos. The ganglia were then placed in a solution of 0.25% trypsin (Sigma) and Puck's balanced saline. After 30 min. incubation, the ganglia were transferred to a tube of neuron medium and dissociated with gentle trituration. Cells were counted with a hemocytometer and plated onto the substrates at a density of 5.2×10^3 cells/cm^2. DRG neurons were maintained in neuron medium (F12 base) and in an incubator set at 37 °C and 5% CO_2. Neurons were sustained for 48 h prior to immunocytochemistry processing. Cocultures of Schwann cells and neurons were made by first allowing plated Schwann cells to reach confluence. Next, DRGs were pipetted onto the Schwann cell coated tubules. Cells were then incubated for an additional 24 h before fixation.

Cultured glia and neurons readily attached to all tubule surfaces. However, to differentiate exterior cell growth from the lumenal surface, a specialized cell culture chamber was fabricated. Briefly, PLLA coated sucrose fibers were placed in a Petri dish and arranged in a parallel fashion. Next, a thin layer of PDMS (∼0.5 mm) was poured over the fibers. The PDMS was allowed to cure for 24 h. Rectangular slots at the fiber ends were then cut out from the PDMS with a scalpel blade. Water was placed in these wells to dissolve the sucrose from the ends. Cells were then pipetted into the exposed wells (DRGs were microinjected into tubules) and allowed to migrate into the lumen. After culturing, cells were fixed with 4% paraformaldehyde, permeabilized with 0.1% Triton X-100 and stained for DNA as described above. For neurofilament staining, primary monoclonal rabbit antineurofilament antibody (1:150 dilution, Sigma) was applied to the cell cultures for 1 h and rinsed with PBS three times. A secondary AlexaFluor 488 conjugated goat antirabbit IgG antibody (1:80 dilution, Invitrogen) was used to couple to the primary NF antibody. Prior to imaging, cells were thoroughly rinsed with PBS to remove unbound fluorophore.

Imaging and Data Analysis. Fluorescence microscopy was conducted on a Nikon Diaphot 300 microscope with a 20X objective. Images were recorded with a CCD camera from Diagnostic Instruments (model 11.2 color mosaic). Digital postprocessing was conducted with ImagePro (Media Cybernetics), PhotoAcute and Photoshop CS3. Recorded fluorescent images were focus stacked (z-stacking, PhotoAcute software) to combine data from multiple image planes. In addition, the background fluorescence for each color channel was subtracted with ImagePro filtering. Color and phase contrast information from each channel was then merged to produce the final composite. For analysis with ImageJ (NIH, http://rsb.info.nih.gov/ij/) 2-D fast Fourier transform (FFT), merged color micrographs were converted to grayscale. Prior to the transformation, images were zero padded (edge masked) with Adobe Photoshop to exclude border induced artifacts. For manual cell tracing, cells were marked by drawing a line along the cell's major axis and obtaining this angle with respect to a reference (tubule direction). The cell deviation angle was defined as the angle between the cell's orientation axis and the reference line. The tubule diameter was then measured locally for each recorded cell.

The external surface topography of hollow PLLA fibers was analyzed with a PSIA XE-120 atomic force microscope (AFM). Fibers were fixed onto a coverslip via application of ethyl-cyanoacrylate. Measurements were acquired in contact or tapping mode using a tip with a force constant of 40 N/m (Budget Sensors) and tip radius of 10 nm. AFM data was processed with XEI software. Pore characterization was carried out by sampling random fields along the external tubule surface. The topographic profiles were then obtained for each pore and the pore diameter was calculated by averaging the major and minor axes of the hole.

For scanning electron microscopy, tubular scaffolds were mounted in PDMS and sputter coated with gold/palladium. Imaging was performed on a JEOL JSM-840 SEM using a 5 kV acceleration voltage at 100−5000× magnification. For freeze fracture, samples were placed in liquid nitrogen and cut with a knife and subsequently imaged.

PLLA tubule cross sections were prepared by mounting the PLLA tubules in Durcupan water soluble resin (EM Sciences). Solid blocks were trimmed and then sectioned with a microtome at 3 μm intervals. Slices were then imaged with a Nikon Diaphot 300 with a 40× objective in phase contrast mode. Recorded images were traced

(14) Thompson, D. M.; Buettner, H. M. *Ann. Biomed. Eng.* **2006**, *34*(1), 161–168.
(15) Sumner, A. J. *Muscle Nerve* **1990**, *13*(9), 801–803.
(16) Campenot, R. B. *Dev. Biol.* **1982**, *93*(1), 13–21.

manually by hand on a light table. For actual tubule measurements, only acquired images (not tracings) were analyzed (ImagePro).

Statistical Methods

All data are reported in the form of mean ± SD. For linear regression and statistical analysis, a p-value of less than 0.05 was considered significant.

Acknowledgment. We would like to thank Michel Schweinsberg for the graphic illustrations.

Supporting Information Available: A time lapse video of the sucrose core (100 μm diameter) dissolving after exposure to distilled water. Water was applied at ~2.4 s into the video. Each second of video corresponds to 10 s of real time. The entire video sequence spans 132 s of total elapsed time. During the dissolution process, small particulates can be seen diffusing across the PLLA tubule wall. This material is available free of charge via the Internet at http://pubs.acs.org.

LA803522F